Plant Omics Journal POJ

POJ 8(5):461-471 (2015) ISSN:1836-3644

Antioxidant enzymes metabolism and cellular differentiation during the developmental stages of somatic embryogenesis in *Torilis japonica* (Houtt.) DC

Abinaya Manivannan[1#], Sonali Jana[2#], Prabhakaran Soundararajan[1#], Chung Ho Ko [1], and Byoung Ryong Jeong[1,2,3,*]

[1]Division of Applied Life Science (BK21 Plus), Graduate School, Gyeongsang National University, Jinju, Korea 660-701
[2]Institute of Agriculture and Life Science, Gyeongsang National University, Jinju, Korea 660-701
[3]Research Institute of Life Science, Gyeongsang National University, Jinju, Korea 660-701

***Corresponding author: brjeong@gmail.com**
[#]Equal contribution as the first author.

Abstract

In the present study, an efficient protocol for high frequency somatic embryogenesis from stem explants of *Torilis japonica* was established. Explants were cultured in Murashige and Skoog (MS) medium containing 0-2.0 mg·L^{-1} 2,4- dichlorophenoxy acetic acid (2,4-D) with or without the combination of indole-3-butyric acid (IBA). The embryogenic callus induction and somatic embryogenesis frequency were measured at four week intervals. The highest embryogenic callus induction (100±0.0%) was achieved in 2.0 mg·L^{-1} 2,4-D and 1.0 mg·L^{-1} IBA. Maximum somatic embryo induction (100±0.0%) was noted on the MS medium augmented with 2.0 mg·L^{-1} 2, 4-D, 1.0 mg·L^{-1} IBA, and 1.0 mg·L^{-1} gibberellic acid (GA_3) with an average of 75.8±3.7 somatic embryos per explant. Scanning electron microscopic investigation and histological analysis demonstrated the systemic development of somatic embryos. Comparatively, the embryogenic callus induction and plantlet conversion stages possessed more total protein and hydrogen peroxide content than other stages. As a consequence, the activities of superoxide dismutase (SOD), guaiacol peroxidase (GPX), ascorbate peroxidase (APX), and catalase (CAT) were also increased during the induction of somatic embryos and bipolar shoot-root axis differentiation stages. Clonal fidelity assessment by random amplified polymorphic DNA (RAPD) fingerprinting and inter simple sequence specific repeats (ISSR) markers displayed the monomorphic banding pattern across the micropropagated plantlets. Thus, the RAPD and ISSR markers validated the genetic homogeneity or the true-to-type nature of the *in vitro* plants.

Keywords: Auxins; Clonal fidelity; Encapsulation; Hydrogen peroxide; ISSR; Native PAGE; RAPD.
Abbreviations: PGRs_Plant growth regulators, 2,4-D_2,4-dichloropheoxyacetic acid, ROS_Reactive oxygen species, GPX_Guaiacol peroxidase, APX_Ascorbate peroxidase, CAT_Catalase, RAPD_Random amplification of polymorphic DNA, ISSR_Inter simple sequence repeat, MS_Murashige and Skoog, IBA_Indole-3-butyric acid, GA_3_Gibberellic acid, SEM_Scanning electron microscopy, SOD_Superoxide dismutase, PAGE_Polyacrylamide gel electrophoresis.

Introduction

Torilis japonica Houtt is an important aromatic medicinal herb belonging to the Apiaceae family widely distributed in East Asia. The fruit of *T. japonica* consists of torilin, a pharmaceutically important sesquiterpene prescribed to treat renal disorders, angiogenesis, cancer, eczema, and inflammation in Chinese medicine and also used as an aphrodisiac in Japan (Juinchi et al., 2002). Previously, torilin has been reported to reverse the multi-drug nature of cancer cells and prevent the invasive ability of human fibrosarcoma cells (Kim et al., 1998; Kim et al., 2001). In addition, the essential oil obtained from the aerial parts of *T. japonica* was effective against pathogenic bacteria such as *Bacillus subtilis*, *Salmonella typhimurium*, and *Listeria monocytogenes* (Cho et al., 2008; Chen et al., 2013). Although, *T. japonica* encloses several pharmaceutical benefits, the conventional propagation of this plant was hindered by poor seed setting, improper pollination, sterility, and under developed flowers, which are the most prevalent problems encountered in the Apiaceae family (Richa et al., 2014). Hence, the development of *in vitro* propagation techniques can rectify the aforementioned difficulties. Moreover, micropropagation by means of somatic embryogenesis offers the possibility for the large scale clonal propagation of *T. japonica* with elite qualities in short period.

Somatic embryogenesis is one of the complex developmental processes in plants. In general, the development of somatic embryos occurs from the somatic cells without fusion of gametes that pave the way for mass propagation of true-to-type plants (Bhojwani and Razdan, 1996). During somatic embryogenesis, the cells may undergo various genetic, proteomic, and biochemical changes (Singla et al., 2007). Application of plant growth regulators (PGRs) either induces somatic embryogenesis either directly from the explants or indirectly from the embryogenic callus. Several studies suggest that the synthetic auxin, 2,4-D is an efficient and effective hormone for somatic embryo induction (Raju et al., 2013). In general, somatic embryogenesis can be considered as the stress responses that occur due to the auxin mediated signaling that enhances the embryogenic competence of the cells. The stress signaling directed by 2,4-D activate the gene expression and protein synthesis responsible for somatic embryogenesis (Mihaljević et al., 2011). Hence, 2,4-D alone or in combination with other plant growth regulators is frequently used in somatic

embryogenesis in many plants (Rathore et al., 2015). However, during reprogramming of somatic cells for embryogenesis several signaling molecules are involved. Among the signaling molecules, the reactive oxygen species (ROS) such as H_2O_2 mediated signaling plays an important role (Zhang et al., 2010). H_2O_2 is one of the vital signaling molecules entailed in the process of differentiation, growth, and development of plants (Kairong et al., 1999). In addition H_2O_2 also acts as a major hallmark of oxidative stress. Therefore, plants have a constitutive effect over the H_2O_2 accumulation i.e., stimulation of defensive antioxidants to scavenge the excess H_2O_2 (Christou et al., 2014). Antioxidant enzymes such as guaiacol peroxidase (GPX), ascorbate peroxidase (APX), and catalase (CAT) are primarily associated with H_2O_2 elimination (Tiryakioglu et al., 2006). Even though, the implication of ROS metabolism with respect to physiological process has been dealt for decades still the underlying metabolic networks remain cryptic.

Therefore, the current study has attempted to investigate the somatic embryogenesis process in *T. japonica* and the consequent biochemical changes that occur during the induction, development, and germination of somatic embryos. Additionally, the present endeavor has also attempted to demonstrate the sodium alginate encapsulation method for synthetic seed production. Moreover, the genetic homogeneity of the *in vitro* plantlets were validated using random amplified polymorphic DNA fingerprinting (RAPD) and inter simple sequence repeat (ISSR) markers.

Results and discussion

Induction and development of somatic embryos

The surface sterilized stem explants inoculated on the auxin augmented Murashige and Skoog (MS) medium bulged at the cut ends within two weeks denoting the early de-differentiation stage. However, the explants cultured on the hormone free-MS medium necrotized after 3 weeks. In general, auxins are prerequisite for the induction and proliferation of callus, whereas the combination of auxin and cytokinins is required for the re-differentiation of callus into organized structures (Wang et al., 2008). The medium supplemented with 2, 4-D possessed the most effective embryogenic callus induction in both alone or in combination with indole-3-butyric acid (IBA). The explants cultured on the 2,4-D medium formed brownish friable embryogenic callus. The greatest embryogenic callus induction percentage (100.0±0.0 %) was achieved in medium with 2.0 $mg \cdot l^{-1}$ 2, 4-D and 1.0 $mg \cdot l^{-1}$ IBA (Table 1). Despite the presence of various auxins, 2,4-D has been widely employed for the induction of somatic embryogenesis in several species (Brown et al., 1995). According to Skupa *et al*. (2014) 2, 4-D creates a time-limited endogenous auxin-maxima or an optimal auxin shock that leads to the induction of somatic embryos. Furthermore the inclusion of IBA along with 2,4-D could have synergistically increased the endogenous auxin stress that led to the enhancement of embryogenic potential of the explants. Similarly, the positive effect of supplementary auxins like IBA on somatic embryogenesis has been reported by Filippov *et al*., (2006) in wheat.

Subsequently, the embryogenic callus progressed to the induction of asynchronous somatic embryos on somatic embryo development medium containing gibberellic acid (GA_3) (Fig. 1A, B). The maximum somatic embryo induction frequency (100.0±0.0%) and highest number of somatic embryos per explant (75.8±3.7) were achieved on MS medium fortified with 2.0 $mg \cdot L^{-1}$ 2,4-D, 1.0 $mg \cdot l^{-1}$ IBA, and 1.0 $mg \cdot l^{-1}$ GA_3 (Table 2). Furthermore, globular embryo proceeded to all the stages of somatic embryo such as heart, torpedo, and cotyledonary stages on the same medium. The role of GA_3 in somatic embryo induction as well as conversion has been reported in many plants such as grapevine cvs. (Lopez-Perez et al., 2006), *Campanula punctata* (Sivanesan et al., 2011), and *Catharanthus roseus* (Dipti and Mujib, 2014).

For plantlet conversion, the late cotyledonary stage embryos were transferred to half strength MS medium supplemented with 1.0 $mg \cdot l^{-1}$ GA_3. After 2 weeks somatic embryos with distinct bipolar structure turned to green color confirming plantlet conversion (Fig. 1C, D). The plantlets were then transferred to hormone free MS medium and cultured for 4 weeks (Fig. 1E, F). The somatic embryo-derived plantlets with well-developed root systems were transferred to a glasshouse for acclimatization. The plants hardened in a glasshouse grew well with 96±0.4% survival ratio (Fig. 1G).

Ultra structural authentication of somatic embryos using scanning electron microscopy (SEM)

The morphological observations of somatic embryos at different stages using SEM were illustrated in Fig 2. The late heart shape and early torpedo stages of distinctly separated embryos were apparent on the SEM micrograph (Fig. 2A). Comparatively, higher number of torpedo and cotyledonary embryos was identified during SEM analysis than globular and heart stage embryos. In Fig. 2B and C, the prominent morphological view of late torpedo stage and mature torpedo stage embryos progressing to the early cotyledonary stage of embryogenesis was noticed. In addition, the asynchronous occurrence of somatic embryos on the surface of the embryogenic callus as nodular protuberance were observed on the scanning electron micrograph (Fig. 2D). The occurrence of cotyledonary embryo clusters with conspicuous bipartite cotyledons evident the progression of somatic embryos from late somatic embryogenesis stage to early plantlet conversion stage (Fig. 2E). Similar morphological features of somatic embryos were examined in *Coriadrum sativum* (Mujib et al., 2014).

Histological examination of systemic cellular differentiation during somatic embryogenesis

The transverse section of embryogenic callus with somatic embryos indicated the presence of small, vacuolated, and dense cells in embryogenic callus (Fig. 3A). It has been noted that the differentiation of embryogenic cells occurred after several mitotic divisions. The initial embryogenic cells constituted the proembryonal complex or the origin site of somatic embryo. In globular and heart stage embryos, the matrix of mesocotyl meristematic cells bounded by the protoderm was observed (Fig. 3B, C). The periclinal and anticlinal divisions of epidermal and subepidermal cells of scutellum led to the formation of rigid cells bounding the meristematic zone (Fig. 3 D, E). Similar observations have been recorded in barley (Nonohay *et al*., 1999). Subsequent development of the procambial cells was evident during the development of somatic embryo.

Generally, initial stages of histo-differentiation are attributed by the formation of protoderm (Yeung, 1995). The shoot and root apical meristems with elongated vascular cells were prominent during the cotyledonary stage representing the establishment of vascular connections between shoot and root primodia (Fig. 3F, G). The shoot and root axis differentiation were distinct in the cotyledonary stage, in which the root apical meristem harboring pool of actively proliferating cells around the quiescent center, calyptrogen, and the root cap were observ-

Table 1. Effects of auxins on the induction of embryogenic callus in *T. japonica.*

PGRs		Embryogenic callus (%)
2,4-D ($mg \cdot l^{-1}$)	IBA ($mg \cdot l^{-1}$)	
0.1	0.0	[z]7.6±0.54 g
0.5	0.0	28.8±1.09f
1.0	0.0	56.8±1.30d
2.0	0.0	95.6±3.43b
0.0	0.1	0.0±0.00h
0.0	0.5	0.0±0.00h
0.0	1.0	0.0±0.00h
0.0	2.0	25.9±1.30f
1.0	0.5	48.2±2.48e
1.0	1.0	58.9±2.58d
2.0	0.5	75.4±4.50c
2.0	1.0	100.0±0.0a

Data are the mean ± SE from three replicates. [z]Mean separation within columns by Duncan's multiple range test at $p \leq 0.05$.

Fig 1. Somatic embryogenesis in *T. japonica.* **(**A) Occurrence of repetitive somatic embryos in stem explant. (B) Tuft of globular embryos emerging from embryogenic callus. (C-E) Regeneration of plantlets from somatic embryos. (F) Mature plantlets in hormone free MS medium. (G) Acclimatized plants in glasshouse.

ed clearly (Fig. 3F). The mature embryos displayed bilateral symmetry with intensely stained apical meristems. The cotyledonary tissues were composed of a distinct protodermis, parenchyma, and vascular connections. In addition the proximal region of the cotyledons consisted of higher number of parenchymatous cells than the distal end (Fig. 3H). Thus the histological analysis has aided a deeper insight into the development of somatic embryo in *T. japonica*.

Sodium alginate mediated- encapsulation of somatic embryos

Embryos embedded in 3 % sodium alginate and hardened for 30 min in 100 mM $CaCl_2.2H_2O$ produced easy to handle, uniform sized stiff beads (Fig. 4A, B, Fig. 5). The smooth texture of synthetic seeds allowed maximum germination percentage (96±0.11 %) on hormone free half strength MS medium containing 0.1 % activated charcoal (Table 3). The synthetic seed germination was noted after 7 days of inoculation (Fig. 4C, D). Even though 4 % sodium alginate encapsulation produced spherical beads, because of dense coat the germination frequency of synthetic seeds was affected. Several previous findings suggest that the optimal concentration of sodium alginate for encapsulation varies among different species. For example the successful encapsulation of somatic embryo has been achieved with 1% sodium alginate in *Acca sellowiana* (Cangahuala-Inocente et al., 2007) whereas 6% alginate encapsulation has proven to be optimal for *Valeriana wallichii* DC (Mathur et al., 1989). Concordantly, Redenbaugh *et al* (1987) suggested the role of capsule as nutrient reservoir for the encapsulated embryo that aids in its survival and germination. Similarly the differential germination response noted upon the varying encapsulation time could be due to the synergistic effects of alginate and calcium concentrations. According to Ipeckci and Gozukirmizi (2003), the germination of synthetic seeds was greatly influenced by the calcium chloride exposure time and capsule texture. Thus the current encapsulation criteria can provide practical means for the extensive commercial production of synthetic seeds and long term storage of embryos of this pharmaceutically important species.

Biochemical changes during somatic embryo development
Analysis of total protein and intra cellular H_2O_2 content

The total protein content was significantly increased in the embryogenic callus after two weeks of inoculation and decreased with embryo development. However the protein contents were high during the plantlet conversion period (Fig 6A). Modulation in the protein content can be due to different metabolic processes involved in the somatic embryo development (Neves et al., 2003). Similarly, the greatest hydrogen peroxide content has been identified during embryogenic callusing stage and in early plantlet conversion stage (Fig 6B). Concordantly, the higher H_2O_2 level induced somatic embryogenesis in *Lycium barbarum* L. (Kairong et al., 2002). H_2O_2 can act as a cellular messenger involved in the induction and regulation of embryogenesis specific gene expression and protein synthesis in plants (Li et al., 2009). Reports also suggest that the H_2O_2 is a down-stream component in auxin-mediated signaling pathway (Konieczny et al., 2014) that possibly enhanced the embryogenic competence of the

Table 2. Somatic embryo induction (%) and number of somatic embryos obtained in *T. japonica* after four weeks of culture.

PGRs			Somatic embryo induction (%)	Number of somatic embryos per/explant
2,4-D ($mg \cdot l^{-1}$)	IBA ($mg \cdot l^{-1}$)	GA_3 ($mg \cdot l^{-1}$)		
1.0	0.5	0.5	[z]5.8±0.83f	7.8±2.16g
2.0	0.5	0.5	23.5±2.0d	28.3±0.5d
1.0	1.0	0.5	14.5±1.9e	11.2±1.3f
2.0	1.0	0.5	48.6±1.3c	40.7±1.7c
1.0	0.5	1.0	21.3±1.4d	20.4±0.3e
2.0	0.5	1.0	84.8±1.1b	52.1±1.1b
1.0	1.0	1.0	45.7±2.1c	31.8±2.2d
2.0	1.0	1.0	100.0±0.1a	75.8±3.7a

Data are the mean ± SE from three replicates. [z]Mean separation within columns by Duncan's multiple range test at $p \leq 0.05$.

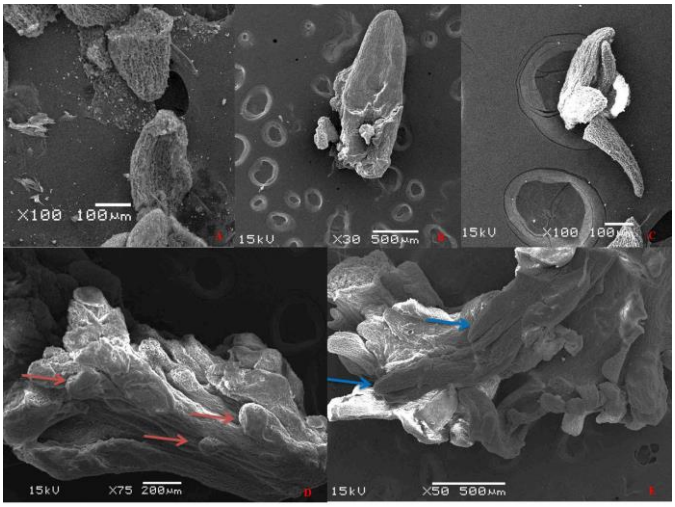

Fig 2. Scanning electron micrographs of somatic embryos. (A-C) Different stages of somatic embryos from late heart to torpedo stages. (D) Cluster of asynchronous somatic embryos with red arrows indicating protruding somatic embryos. (E) Clump of late cotyledonary stage somatic embryos with distinct bipartite cotyledon structure was denoted by blue arrows.

explant. This could be a coincidental factor for the occurrence of higher amount of H_2O_2 in the early stage of somatic embryo induction. However, the H_2O_2 level decreased with the somatic embryo development and increased during plantlet conversion.

Antioxidant enzymes metabolism during somatic embryogenesis

Excess accumulation of ROS can disturb the redox homeostasis, normal physiological activities and cellular metabolism. In order to maintain the balance of intracellular ROS content, plant possesses the antioxidant system to manage the surplus ROS level. Concordantly, the activities of antioxidant enzymes such as SOD, GPX, CAT, and APX were increased during the embryo induction stage and plantlet conversion stage in accordance with the intracellular H_2O_2 level (Fig 7). SOD is the primary enzyme which dismutase the superoxide to H_2O_2 (Manivannan et al., 2015). In the present result, the increase in SOD activity is consistent with the elevated levels of H_2O_2 in the early and later stages of somatic embryogenesis. Moreover, the SOD active staining revealed the occurrence of single band corresponding to Mn-SOD and two bands denoting Cu-Zn isoforms throughout the developmental stages (Fig. 7A). The involvement of SOD in the early stages of somatic embryo development has been reported in several plants including *Lycium barbarum* L., *Larix leptolepis*, and *Musa spp* (Kairong et al., 1999, Zhang et al., 2010, Ma et al., 2012). The H_2O_2 generated by the SOD dismutation reaction will be further detoxified into H_2O and molecular oxygen by other antioxidant enzymes. Thus, the changes in the endogenous H_2O_2 content during the somatic embryogenesis subsequently triggered a cascade of H_2O_2 scavengers such as GPX, CAT, and APX enzymes to eliminate the excess H_2O_2 (Fig 7B-D). Three GPX isoforms were detected in the somatic embryos but the expression of the GPX3 was distinct in the EC and P stages (Fig 7B). GPX catalyzes the reduction of H_2O_2 to H_2O by utilizing several substrates as the electron donors and also play vital roles in somatic embryogenesis (Wang et al., 2009; Ma et al., 2012). In accordance with SOD and GPX, catalase also displayed higher activity in EC and P stages. Moreover, the active staining displayed the presence of two isoforms of CAT enzyme in which the expression of CAT2 isoform was higher in the EC and P stages (Fig. 7C). In similar manner with GPX, CAT prevents the formation of free radicals by reducing the H_2O_2 into water and dioxygen (Ma et al., 2012). Active staining and activity analysis of APX displayed the similar trend with the other antioxidant enzymes (Fig. 7D). Furthermore, the elevated levels of H_2O_2 in the P stage can also be correlated with the higher metabolic activities of chloroplast and mitochondria. Since the physiological process such as respiration and photosynthesis which involves chloroplast and mitochondria, the major sources of intracellular H_2O_2 (Li et al., 2009). Studies suggested the existence of a link between the ROS metabolism and the totipotency of plants. For instance, in tobacco the reduction in ROS concentration has declined the totipotency (Papadakis et al., 2001). Moreover the lower level of H_2O_2 during the developmental stages of somatic embryo could be due to the emergence of meristematic and vascular tissues because in

Table 3. Effect of different concentrations of sodium alginate and calcium chloride on the germination frequency (%) of *Torilis japonica* Houtt. synthetic seeds.

Sodium alginate (%)	Calcium chloride (mM)	Germination (%)
3	75	[z]82±0.62b
3	100	96±0.11a
4	75	77±0.58c
4	100	85±0.74b

Data are the mean ± SE from three replicates. [z]Mean separation within columns by Duncan's multiple range test at $p \leq 0.05$.

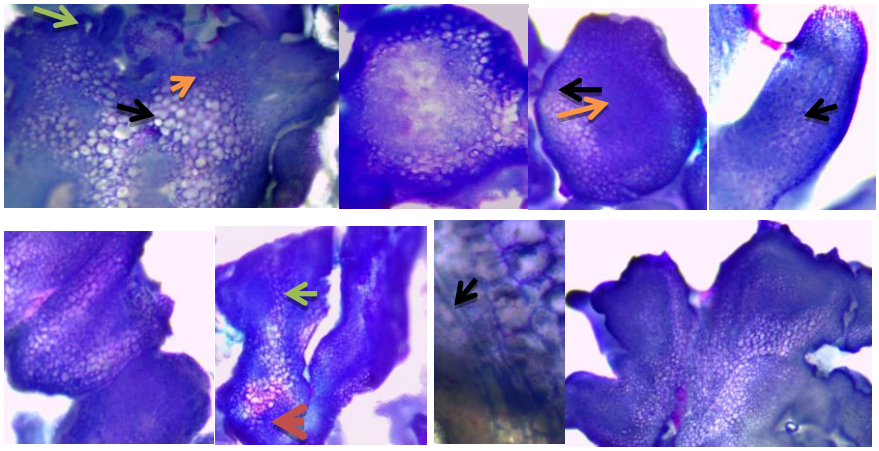

Fig 3. Histological analysis of somatic embryogenesis. (A) Transverse section of embryogenic callus containing somatic embryos, the middle black arrow represents the meristematic cells, orange arrow indicates the proembryonal region, and the green arrow shows the somatic embryo. (B) Globular stage somatic embryo. (C) Early torpedo stage embryo with distinct protoderm (black arrow) and procambial cells (orange arrow). (D) Late torpedo stage embryo with elongated cambial cells (black arrow). (E) Early heart stage embryo. (F) Cotyledonary stage embryo with prominent shoot apical meristem (green arrow) and root apical meristem (brown arrow). (G) Elongated vascular cells in cotyledonary embryos represented by black arrow. (H) Somatic embryos with dense cambial cells in the middle and apical meristems in proximal and distal ends.

strawberry the H_2O_2 content decreased with the development of meristemoids and vascular tissues (Tian et al., 2003). Similar observations have been recorded during the somatic embryogenesis of *Astragalus adsurgens* (Luo et al., 2001). Thus, our results demonstrate the importance of H_2O_2 during the induction and regulation of somatic embryogenesis along with the modulation in antioxidant enzyme activities.

Clonal fidelity assessment by RAPD fingerprinting and ISSR markers

Genetic integrity of the somatic embryo derived plants and the mother plant was evaluated using twenty RAPD and ten ISSR markers. The random decamers employed in our study for RAPD analysis have been applied successfully for assessing the polymorphism in *Paeonia lactiflora* (Lim et al., 2013) and *Viola pilosa* (Soni and Kaur, 2014). RAPD results revealed the true-to-type nature of the somatic embryo derived plants by forming monomorphic banding pattern on compared with the mother plant. RAPD primers resulted in 117 scorable bands and the total number of bands by individual primers has been listed in Table 4. The primers A02, A04, A05, A09, and A13 produced consistent 9 monomorphic bands. The size of the amplicons ranged from 200-1500 base-pairs. The monomorphic banding profiles generated by the random primers A02, A14, A12, and A20 across the mother plant and seven randomly selected somatic embryo-derived plants have been shown in Fig.8. Detection of genetic stability using RAPD fingerprinting has been successful in several species, namely *Elaeis guineensis* Jacq (Rival et al., 1998), *Asparagus officinalis* (Raimondi et al., 2001), and cucumber (Elmeer et al., 2009). Although, RAPD fingerprinting has been widely applied to validate the clonal fidelity of the micropropagated plants because of its simplicity and robustness, the dominant and non-sequence specific nature of the RAPD primers decreases the reproducibility of the technique (Agarwal et al., 2015). Therefore, RAPD fingerprinting has to be supported by other DNA markers such as ISSR for accurate genetic stability analysis (Agarwal et al., 2015). ISSR markers are highly reproducible, semi arbitrary, dominant, and more stringent than RAPD markers (Agarwal et al., 2015). In the present study, the utilization of ISSR markers authenticated the genetic homogeneity of the *in vitro* plants with the mother plant. The ISSR banding profile generated by the primers UBC 812, UBC 827, UBC 855, and UBC 889 were shown in Fig.9. All the ISSR primers yielded a unique set of monomorphic amplicons ranging from 200-1000 bp (Table. 5). Among the UBC primers, UBC-834 resulted in maximum number of fragments (17) followed by UBC-859. The evaluation of genetic stability in micropropagated plants using ISSR markers has been reported in several species (Ramakrishnan et al., 2014; Agarwal et al., 2015). Moreover, the molecular marker based clonal fidelity assessment results were summarized in Table 6. Overall, the RAPD and ISSR markers validated the genetic homogeneity of the *in vitro* raised plants and also authenticated the somatic embryo derived plants remain free from somaclonal variations.

Materials and Methods

Plant materials

Stem segments of *T. japonica* were collected from the 6 months old plants grown in a glasshouse at Gyeongsang National University, Jinju, Korea. The excised explants were washed thoroughly under running tap water with few drops of Tween 20 for 10 min. For surface sterilization, the explants were decontaminated with 70 % (v/v) ethanol for 5 min, 1.5 % (v/v)

Table 4. Total number of amplicons and amplicon size assayed by RAPD fingerprinting.

Primer	Sequence (5' - 3')	Total number of amplicons	Size range (base pairs)
A01	CAGGCCCTTC	6	1000-200
A02	TGCCGAGCTG	9	1000-200
A03	AGTCAGCCAC	7	1000-500
A04	AATCGGGCTG	9	1500-200
A05	AGGGGTCTTG	9	1500-400
A06	GGTCCCTGAC	6	1200-400
A07	GAAACGGGTG	6	900-400
A08	GTGACGTAGG	7	900-300
A09	GGGTAACGCC	9	1500-300
A10	GTGATCGCAG	7	1500-200
A11	CAATCGCCGT	6	1000-400
A12	TCGGCGATAG	6	1500-300
A13	CAGCACCCAC	9	1000-100
A14	TCTGTGCTGG	7	1500-200
A15	TTCCGAACCC	5	1500-500
A16	AGCCAGCGAA	4	700-400
A17	GACCGCTTGT	3	1000-500
A18	AGGTGACCGT	3	1000-300
A19	CAAACGTCGG	3	800-400
A20	GTTGCGATCC	4	1500-300
Total number of bands		117	

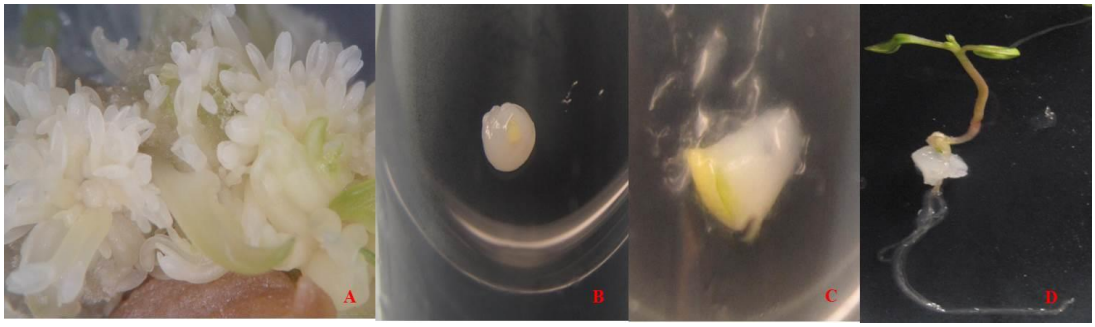

Fig 4. Sodium alginate encapsulation and germination of somatic embryo. **(**A) Clump of torpedo stage embryos before encapsulation. (B) Alginate-encapsulated bead containing somatic embryo. (C) Germination of embryo after 7 days. (D) Plantlet obtained from synthetic seed.

sodium hypochlorite (NaClO) for 5 min followed by 6-7 washes with distilled water. After the surface sterilization process the explants were blot dried in a sterilized filter paper and inoculated onto the medium. The culture medium consisted of the Murashige and Skoog (MS) basal salts and vitamins (Murashige and Skoog, 1962) supplemented with 3 % (w/v) sucrose, and solidified with 0.8 % (w/v) agar. The pH of the medium was adjusted to 5.75 before autoclaving at 121 ℃ for 15 min. Plant growth regulators (PGRs) were added to the basal medium prior to pH adjustment. The gibberellic acid (GA_3) was filter sterilized and added to the autoclaved medium.

Induction and development of somatic embryos

Explants (1-2 cm in length) were cultured on the MS medium supplemented with various concentrations and combinations of 2,4- dichlorophenoxyacetic acid (2,4-D) and indole-3-butyric acid (IBA) alone or in combinations. The PGR-free medium was used as the control. Five explants were placed in each petridish containing 20 ml of the MS medium and maintained for 15 days at 25 ℃ in darkness, and then exposed to light of 45 µmol $m^{-2}s^{-1}$PPFD for a daily 16/8 h light/dark cycle. The frequency of somatic embryo formation was determined by calculating the number of explants forming somatic embryos from the total number of the cultured explants. For somatic embryo germination, the cotyledonary stage embryos were separated from the explants and cultured on half strength MS medium supplemented with 0.5 or 1.0 $mg \cdot l^{-1}$ GA_3. Embryo germination was calculated after 30 days as the percentage of number of converted embryos per total number of somatic embryos.

Plantlet conversion and acclimatization

Healthy regenerated plantlets with well-developed roots were removed from culture vessel, washed thoroughly with running tap water. The plants were then transferred to 12-cell plug trays containing a commercial greenhouse medium (Tosilee medium, Shinan Precision Co., Jinju, Korea) and maintained in a controlled growth chamber. The plants were fertigated every alternative day. After 2 weeks the plants were transferred to 10 cm pots and hardened in a glasshouse at Gyeongsang National University, Jinju, Korea, under a normal daylight condition with night/day set temperatures of 27/19°C and 60-70% relative humidity (RH). The survival ratio of the micropropagated plants were recorded after 45 days of acclimatization.

Scanning electron microscopic (SEM) analysis of somatic embryos

The sample preparation and SEM analysis of somatic embryos were carried out according to Mujib *et al* (2014) with minor

Table 5. Total number and size of amplicons generated by ISSR markers.

Primer	Sequence (5' - 3')	Tm (°C)	Total number of amplicons	Size range (base pairs)
UBC-809	AGAGAGAGAGAGAGAGG	42.0	5	700-200
UBC-810	GAGAGAGAGAGAGAGAT	44.0	11	1000-200
UBC-811	GAGAGAGAGAGAGAGAC	38.5	6	900-500
UBC-812	GAGAGAGAGAGAGAGAA	39.0	4	700-200
UBC-827	ACACACACACACACACG	42.0	8	900-400
UBC-834	AGAGAGAGAGAGAGAGYT	42.5	17	1000-400
UBC-855	ACACACACACACACACYT	44.0	5	900-300
UBC-859	TGTGTGTGTGTGTGTGRC	38.5	13	900-300
UBC-881	GGGTGGGGTGGGGTG	43.0	9	1000-300
UBC-889	DBDACACACACACACAC	45.5	7	1000-400
Total number of bands			85	

R= (A, G); Y= (A, C, G); D = (non C); B = (non A)

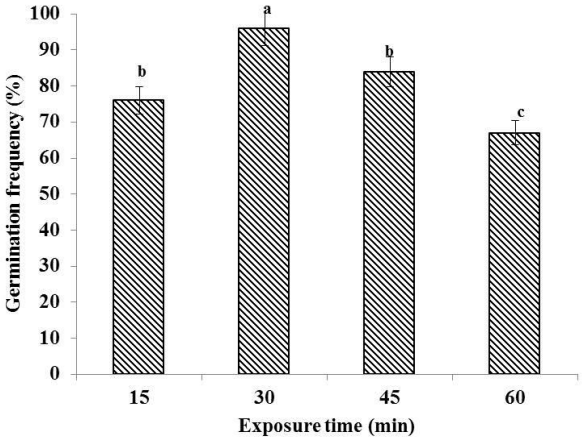

Fig 5. Effect of calcium chloride exposure time on the germination frequency of encapsulated embryos.

Table 6. Summary of clonal fidelity assessment scores of RAPD and ISSR markers

Description	RAPD	ISSR	RAPD +ISSR
Total number of bands scored	117	85	202
Number of monomorphic bands scored	117	85	202
Number of polymorphic bands scored	0	0	0
Number of primers employed	20	10	30
Average number of amplicons per primer	5.85	8.5	6.7

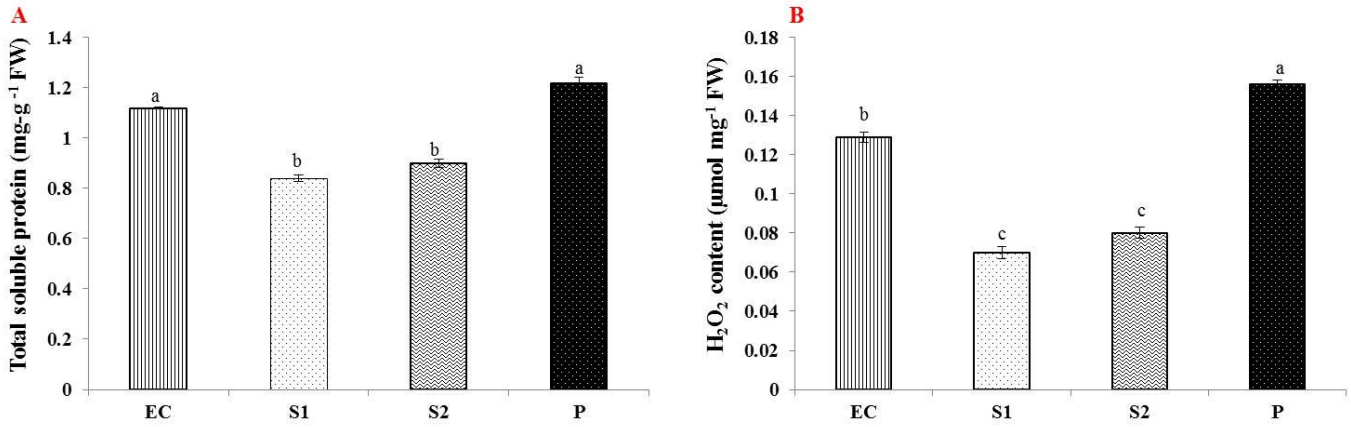

Fig 6. Biochemical analysis of somatic embryos at different stages such as EC-embryogenic callus, S1- two weeks old somatic embryo, S2- four weeks old embryo, and P- two weeks old regenerated plantlet. (A) Total protein content. (B) Hydrogen peroxide content. Data are the mean ± SE from three replicates. Different letters in one measurement indicate treatments are statistically different at $p \leq 0.05$.

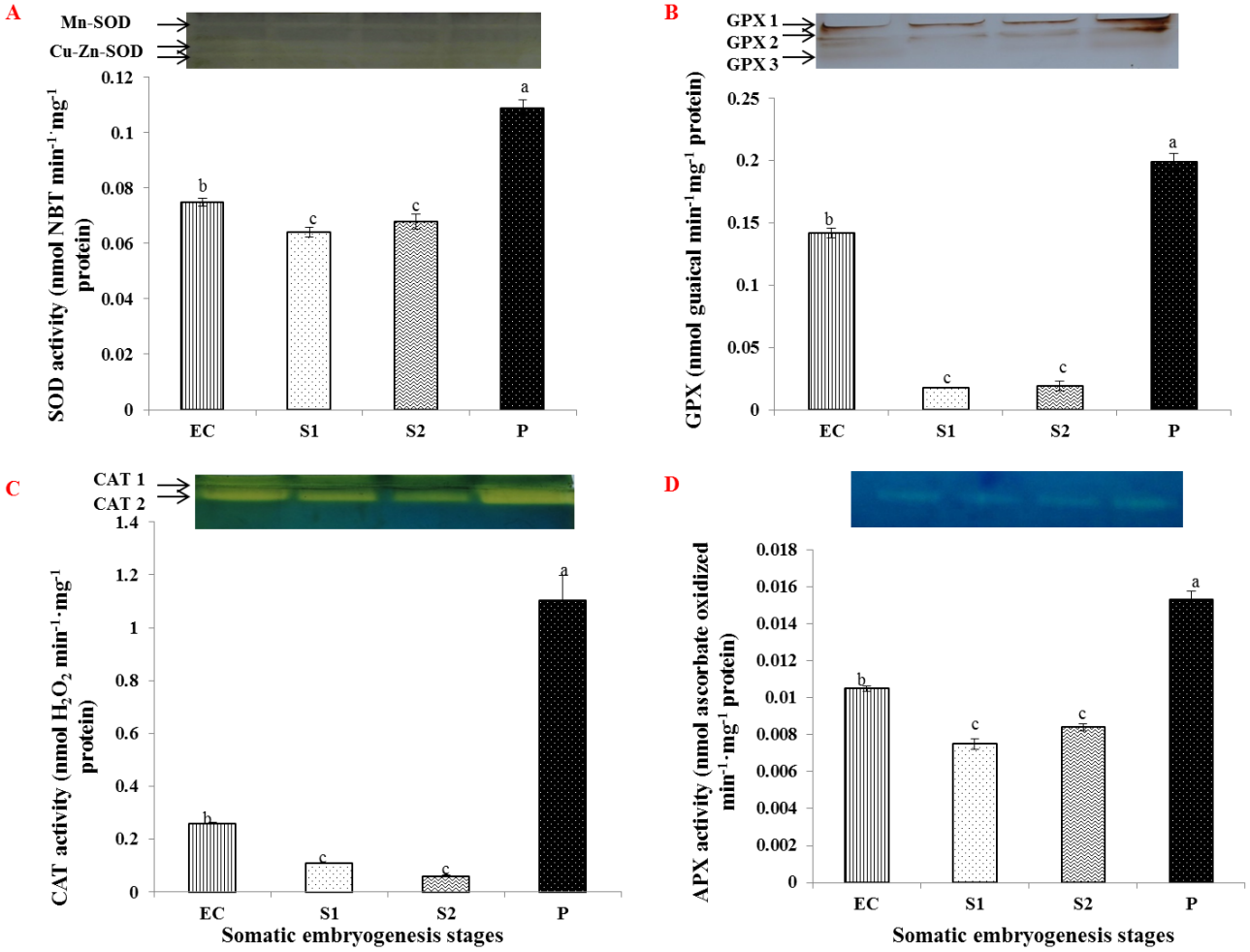

Fig 7. Modulation in the activities of antioxidant enzymes along with active staining localization during different stages such as EC- embryogenic callus, S1- two weeks old somatic embryo, S2- four weeks old embryo, and P- two weeks old regenerated plantlet. (A) Superoxide dismutase (SOD). (B) Guaiacol peroxidase (GPX). (C) Catalase (CAT). (D) Ascorbate peroxidase (APX). Data are the mean ± SE from three replicates. Different letters in one measurement indicate statistical differences at $p \leq 0.05$.

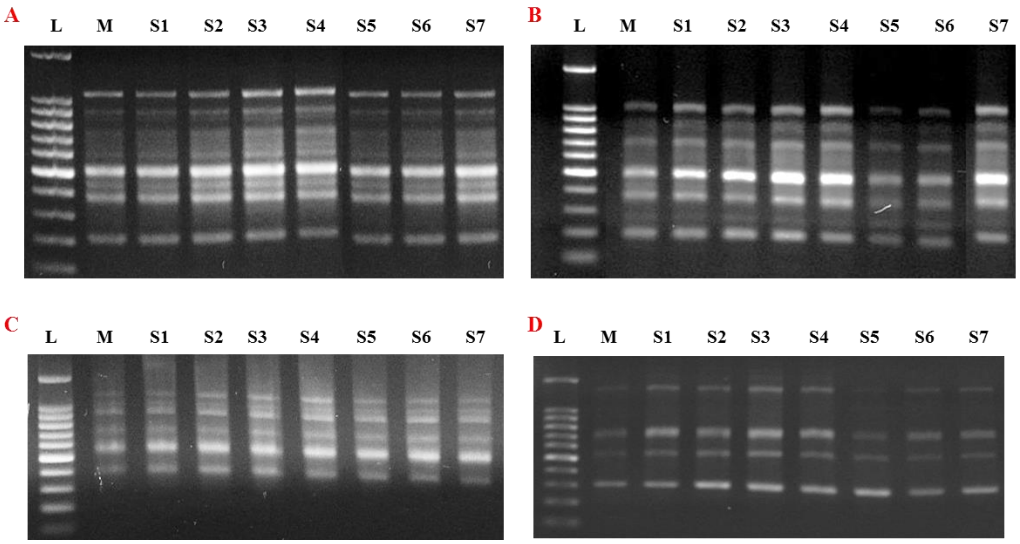

Fig 8. RAPD amplification profile obtained for the primers, (A) A02, (B) A14, (C) A12, and (D) A20. L-refers to DNA ladder, M- represents mother plant and S1-7 refers to seven randomly selected somatic embryo-derived plantlets acclimatized in glasshouse.

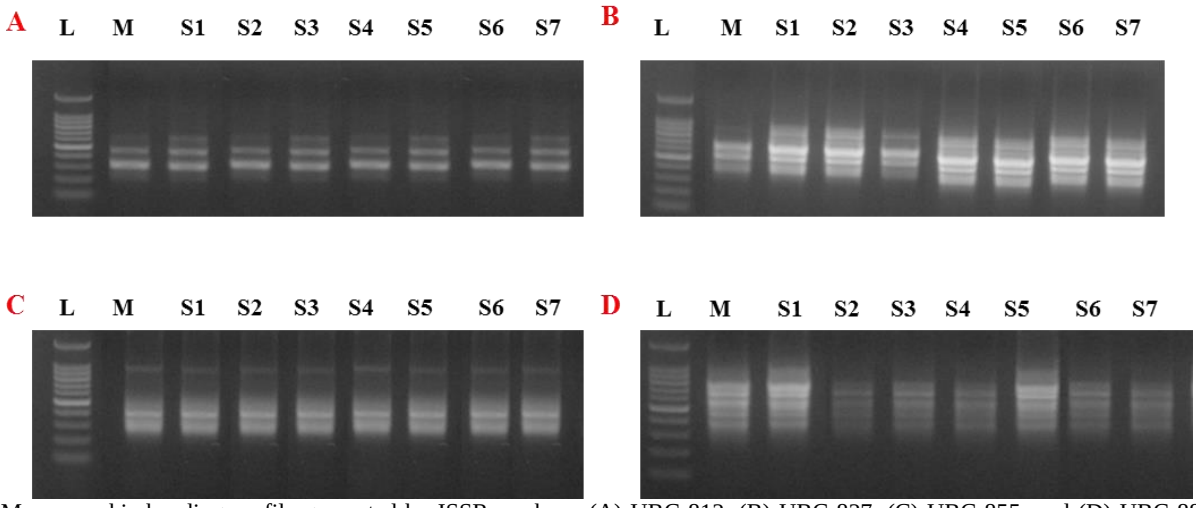

Fig 9. Monomorphic banding profile generated by ISSR markers, (A) UBC-812, (B) UBC-827, (C) UBC-855, and (D) UBC-889. L-refers to DNA ladder, M-represents mother plant and S1-7 refers to seven randomly selected somatic embryo-derived plantlets acclimatized in glasshouse.

modifications. Initially the embryos were fixed in 2.5 % glutaraldehyde for overnight at 4°C and washed with 0.1 M phosphate buffered saline (PBS, pH 7.0). After PBS wash, the samples were fixed in buffered 4 % osmium tetroxide solution (pH-7.0) for 2h at 4°C. Subsequently, the samples were dehydrated in graded series of ethanol (30, 50, 70, 90, and 100 %). After dehydration the samples were dried, gold coated, examined, and photographed under JSM-6380 (JEOL, USA) scanning electron microscope operating at 15-25 kv.

Histological examination of somatic embryos

The histological procedures were performed according to Nic-Can *et al*. (2013). Briefly, somatic embryos were fixed in 10% formaldehyde, 5% acetic acid and 50% ethanol for 48 hr. After fixation the samples were rinsed in phosphate buffer (2mM, pH 7.4) for 5 times followed by dehydration in graded series of ethanol (10, 30, 50, 70, 85, 96, and 100%) and vacuum dried at 10 min interval. The whole set up was maintained at 4°C for 1 h and repeated again. For sectioning, the samples were embedded in resin and segmented to 5 µm using Plant microtome MTH1 and the sliced tissues were stained with 0.01 % toluidine O. The microscopic observations were performed using Nikon-Y-TV55 light microscope.

Estimation of hydrogen peroxide

For the biochemical analysis, embryogenic callus (EC), two weeks old somatic embryo (S1), four weeks old embryo (S2), and two weeks old regenerated plantlet (P) were employed. The endogenous H_2O_2 level was measured at 390 nm using the standard H_2O_2 calibration curve according to Alexieva *et al*. (2001).

Estimation of antioxidant enzymes activity and native PAGE analysis

To determine the antioxidant enzymes activity, 0.1 g of tissue was homogenized in 50 mM phosphate buffer (pH 7.0) containing 1 mM EDTA, 0.05 % triton X, and 1 mM polyvinylpyrolidone (PVP). Then the homogenate was centrifuged at 13,000 rpm for 20 min at 4 °C and the supernatant was used for determination of antioxidant enzymes activity.

Sodium dismutase (SOD), catalase (CAT), ascrobate peroxidase (APX), and guaiacol peroxidase (GPX) enzyme activities were estimated by following the protocols of Shekhawat et al. (2010). The total protein content was estimated at 595 nm according to Bradford method using bovine serum albumin as standard (Bradford, 1976).

The native–PAGE analysis of the antioxidant enzymes and the localization of enzyme isomers were performed according to Shah and Sareeta (2012). Briefly, the electrophoresis was carried out in 10 % separating and 4 % stacking gel in 4 °C for 4 h at 80 volts with Tris-glycine (pH 8.3) running buffer. The samples (30 µg protein) were prepared with the laemmli buffer containing glycerol and bromophenol blue (0.02 %). For the GPX active staining, the gels were washed with distilled water after the run and incubated for 20 min in 50 mM Tris-HCl buffer (pH 6.8) with 20 mM guaiacol and 20 mM H_2O_2. The SOD isozymes were visualized by immersing the gel in SOD reaction mixture (EDTA, NBT, methionine, riboflavin) for 15 min in dark followed by light irradiation for 30 min. The SOD isozymes were localized as the colorless bands. APX was localized by flooding the gel with 50 mM phosphate buffer (pH 6.4) containing 4 mM ascorbic acid and 4 mM H_2O_2 for 15 min. The gel was stained with 0.1% ferrocyanide and 0.1% ferricchloride prepared in 1.25 N HCl for 5 min and the APX isozyme was visualized as colorless band on Prussian blue background. The CAT enzyme was observed as a colorless band on green background when the gel was incubated in 50 mM phosphate buffer (pH 7.0) with 5 mM H_2O_2. After 10 min the gel was transferred to staining solution containing 2% ferric chloride and 2% potassium ferric cyanide.

Encapsulation of somatic embryos

For encapsulation, somatic embryos in torpedo stage (2-3 mm) were embedded into 3 or 4% sodium alginate (Sigma Aldrich, USA) prepared in liquid MS medium and dispersed in 75 or 100 mM calcium chloride. The beads were hardened in $CaCl_2.2H_2O$ for 15-60 min and washed with distilled water. The washed beads were blot dried in filter paper and inoculated onto the half-strength MS medium containing 0.1% activated charcoal. The germination frequency was calculated after 3 weeks of inoculation. The germinated synthetic seeds were allowed to develop into mature plantlets and acclimatized as mentioned above.

Clonal fidelity assessment of in vitro plants using RAPD and ISSR markers

The genomic DNA was isolated from the leaf sample of randomly selected plants hardened in glasshouse using plant DNA extraction kit (iNtRON Biotechnology, Seongnam, Korea). The clonal fidelity of the micropropagated plants were detected using randomly amplified polymorphic DNA (RAPD) fingerprinting assay. The assay was carried out with 20 random decamers (Enotech Co., Daejeon, Korea) as listed in Table 4. For genetic stability assessment using ISSR markers, ten UBC primers shown in Table 5 were employed. For all PCR reactions, the reaction mixture consisted of a total volume of 20 µl with 1X PCR buffer, 2.5 mM dNTPs, and 2.5 U *Taq* DNA polymerase (iNtRON's Maxime PCR Pre-mix, Seongnam, Korea) with 1 µl primer, and 2 µl DNA. The PCR amplification was performed in a thermal cycler (Gene Amp PCR system 9700, Applied Biosystems, Foster City, CA, U.S.A.). The amplification profile consisted of initial denaturation (5 min at 94°C),denaturation (1 minute at 94°C), annealing (1 minute at 33°C for RAPD primers and different annealing temperatures employed for individual ISSR primers were listed in Table 5), extension (1 minute at 72°C), and final extension (10 minutes at 72°C) with 30 cycles. Amplified PCR products were separated on 1.5 % agarose gel and photographed under UV light in a gel documentation system.

Statistical analysis

In each treatment, 30 explants were used and the experiment was repeated thrice. Data were statistically analyzed by analysis of variance (ANOVA) followed by Duncan multiple range test at 5% probability level. Data analysis was performed using SAS computer package (SAS Institute Inc., Cary, NC, USA).

Conclusions

The present work has successfully established an efficient protocol for high frequency somatic embryogenesis in *Torillis japonica* Houtt. In addition, SEM analysis and histological observations demonstrated the development of somatic embryos. Moreover, the biochemical modulation during the induction and development of somatic embryos revealed the vital involvement of H_2O_2 and antioxidant enzymes. Further, the efficient alginate encapsulation for synthetic seed production was demonstrated and the genetic homogeneity of the *in vitro* plants was assessed using RAPD fingerprinting and ISSR markers. In future, the current endeavor can be extended to determine molecular rationale behind the somatic embryogenesis in pharmaceutically valuable *Torilis japonica* Houtt.

Acknowledgements

Abinaya Manivannan, Prabhakaran Soundararajan, and Chung Ho Ko were supported by a scholarship from the Brain Korea 21 Plus (BK21 plus) Program, Ministry of Education, Korea. The authors are thankful to Dr. Yoo Gyeong Park for statistical assistance.

References

Agarwal T, Gupta A K, Patel A K, Shekhawat N S (2015) Micropropagation and validation of genetic homogeneity of *Alhagi maurorum* using SCoT, ISSR and RAPD markers. Plant Cell Tiss Org Cult. 120(1):313-323.

Alexieva V, Sergiev I, Mapelli S, Karanov E (2001) The effect of drought and ultraviolet radiation on growth and stress markers in pea and wheat. Plant Cell Environ. 24:1337-1344.

Bhojwani SS, Razdan MK (1996) Plant Tissue Culture: Theory and Practice. Elsevier, New York.

Bradford MM (1976) A rapid and sensitive method for the quantitation of microgram quantities of protein utilizing the principle of protein-dye binding. Anal Biochem.72:248-254.

Brown DCW, Finstad KI, Watson EM (1995) Somatic embryogenesis in herbaceous dicots. In: Thorpe TA (ed) In vitro embryogenesis in plants. Kluwer, Dordrecht.

Cangahuala-Inocente GC, Vesco LLD, Steinmacher D, Torres AC, Guerra MP (2007) Improvements in somatic embryogenesis protocol in Feijoa (*Acca sellowiana* (Berg) Burret): induction, conversion and synthetic seeds. Sci Hortic. 111:228-234.

Chen J, Xu XJ, Fang YH, Li S, Zhang YI (2013) Chemical composition and antibacterial activity of the essential oil from the aerial parts of *Torilis japonica*. J Essential Oil Bearing Plants. 16(4):499-505.

Cho WI, Choi JB, Lee K, Chung MS, Pyun YR (2008) Antimicrobial activity of torilin isolated from *Torilis japonica* fruit against *Bacillus subtilis*. J Food Sci. 73(2):37-46.

Christou A, Manganaris GA, Fotopoulos V (2014) Systemic mitigation of salt stress by hydrogen peroxide and sodium nitroprusside in strawberry plants via transcriptional regulation of enzymatic and non-enzymatic antioxidants. Environ Exp Bot. 107:46-54.

Dipti SF, Mujib A (2014) Morphological anomalies in somatic embryo structure in *Catharanthus roseus*: Improving embryo germination by amending plant growth regulators, activated charcoal and sucrose level. Br Biotechnol J. 4:10-20.

Elmeer KMS, Gallagher TF, Hennerty MJ (2009) RAPD-based detection of genomic instability in cucumber plants derived from somatic embryogenesis. Afr J Biotechnol. 8:3219-3222.

Filippov M, Miroshnichenko D, Vernikovskaya D, Dolgov, S (2006) The effect of auxins, time exposure to auxin and genotypes on somatic embryogenesis from mature embryos of wheat. Plant Cell Tiss Org Cult. 84(2):213-222.

Ipekci Z, Gozukirmizi N (2003) Direct somatic embryogenesis and synthetic seed production from *Paulownia elongata*. Plant Cell Rep. 22(1):16-24.

Junichi K, Nobuyuki S, Mituru S, Mitsuo W (2002) Sesquiterpenoids of *Torilis japonica* fruit. Phytochem. 59(8):811-815.

Kairong C, Gengsheng X, Xinmin L, Gengmei X, Yafu W (1999) Effect of hydrogen peroxide on somatic embryogenesis of *Lycium barbarum* L. Plant Sci. 146(1):9-16.

Kairong C, Ji L, Gengmei X, Jianlong L, Lihong W, Yafu W (2002) Effect of hydrogen peroxide on synthesis of proteins during somatic embryogenesis in *Lycium barbarum.* Plant Cell Tiss Org Cult. 68(2):187-193.

Kim MS, Baek JH, Park MT, Sohn TK, Lee JJ, Kim SU, Kim KW (2001) Anti-invasive activity of torilin, a sesquiterpene compound isolated from *Torilis japonica*. Oncol Rep. 8:359-364.

Kim SE, Kim YH, Kim YC, Lee JJ (1998) Torilin, a sesquiterpene from *Torilis japonica*, reverses multidrug-resistance in cancer cells. Planta Med. 64(4):332-334.

Konieczny R, Banaś AK, Surówka E, Michalec Ż, Miszalski Z, Libik-Konieczny M (2014) Pattern of antioxidant enzyme activities and hydrogen peroxide content during developmental stages of rhizogenesis from hypocotyl explants of *Mesembryanthemum crystallinum* L. Plant Cell Rep. 33(1):165-177.

Li SW, Xue L, Xu S, Feng H, An L (2009) Hydrogen peroxide acts as a signal molecule in the adventitious root formation of mung bean seedlings. Environ Exp Bot. 65:63-71.

Lim MY, Jana S, Sivanesan I, Park HR, Hwang JH, Park YH, Jeong BR (2013) Analysis of genetic variability using RAPD markers in Paeonia spp. grown in Korea. Kor J Hort Sci Technol. 31:322-327.

Lopez-Perez AJ, Carreno J, Dabauza M (2006) Somatic embryo germination and plant regeneration of three grapevine cvs: Effect of IAA, GA_3 and embryo morphology. Vitis. 45:141-143.

Luo JP, Jiang ST, Pan LJ (2001) Enhanced somatic embryogenesis by salicylic acid of *Astragalus adsurgens* Pall.: relationship with H_2O_2 production and H_2O_2-metabolizing enzyme activities. Plant Sci. 161(1):125-132.

Ma L, Xie L, Lin G, Jiang S, Chen H, Li H, Takac T, Samaj J, Xu C (2012) Histological changes and differences in activities of some antioxidant enzymes and hydrogen peroxide content during somatic embryogenesis of *Musa AAA* cv. Yueyoukang 1. Sci Hortic. 144:87-92.

Manivannan A, Soundararajan P, Halimah N, Ko CH, Jeong BR (2015). Blue LED light enhances growth, phytochemical contents, and antioxidant enzyme activities of *Rehmannia glutinosa* cultured in vitro. Hortic Environ Biotechnol. 56(1):105-113.

Mathur J, Ahuja PS, Lal N, Mathur AK (1989) Propagation of *Valeriana wallichii* DC using encapsulated apical and axial shoot buds. Plant Sci. 60:111-116.

Mihaljević S, Radić S, Bauer N, Garić R, Mihaljević B, Horvat G, Jelaska S (2011) Ammonium-related metabolic changes affect somatic embryogenesis in pumpkin (*Cucurbita pepo* L.). J Plant Physiol. 168(16):1943-1951.

Mujib A, Tonk D, Ali M (2014) Plant regeneration from protoplasts in Indian local *Coriandrum sativum* L.: scanning electron microscopy and histological evidences for somatic embryogenesis. Plant Cell Tiss Org Cult. 117(3):323-334.

Murashige T, Skoog F (1962) A revised medium for rapid growth and bio assays with tobacco tissue cultures. Physiol Plantarum. 15(3):473-497.

Neves N, Segura-Nieto M, Blanco MA, Sánchez M, González A, González JL (2003) Biochemical characterization of embryogenic and non-embryogenic calluses of sugarcane. InVitro Cell Dev Biol Plant. 39(3):343-345.

Nic-Can GI, López-Torres A, Barredo-Pool F, Wrobel K, Loyola-Vargas VM, Rojas-Herrera R, De-la-Peña C (2013) New insights into somatic embryogenesis: LEAFY COTYLEDON1, BABY BOOM1 and WUSCHEL-RELATED HOMEOBOX4 are epigenetically regulated in *Coffea canephora*. PloS One. 8(8):e72160.

Nonohay JS, Mariath JEA, Winge H (1999) Histological analysis of somatic embryogenesis in Brazilian cultivars of barley, *Hordeum vulgare vulgare*, Poaceae. Plant Cell Rep. 18(11):929-934.

Papadakis AK, Siminis CI, Roubelakis-Angelakis KA (2001) Reduced activity of antioxidant machinery is correlated with suppression of totipotency in plant protoplasts. Plant Physiol. 126(1):434-444.

Raimondi JP, Masuelli RW, Camadro EL (2001) Assessment of somaclonal variation in asparagus by RAPD fingerprinting and cytogenetic analyses. Sci Hortic. 90:19-29.

Raju CS, Kathiravan K, Aslam A, Shajahan A (2013) An efficient regeneration system via somatic embryogenesis in mango ginger (*Curcuma amada* Roxb.). Plant Cell Tiss Org Cult. 112(3):387-393.

Ramakrishnan M, Ceasar SA, Duraipandiyan V, Ignacimuthu S (2014) Efficient plant regeneration from shoot apex explants of maize (*Zea mays*) and analysis of genetic fidelity of regenerated plants by ISSR markers. Plant Cell Tiss Org Cult. 119(1):183-196.

Rathore MS, Paliwal N, Anand KV, Agarwal PK (2015) Somatic embryogenesis and in vitro plantlet regeneration in *Salicornia brachiata* Roxb. Plant Cell Tissue Organ Cult. 120(1):355-360.

Redenbaugh K, Slade D, Viss P, Fujii JA (1987) Encapsulation of somatic embryos in synthetic seed coats. HortScience. 22:803-809.

Richa D, Shekhawat GS, Alam A (2014) Improved protocol for somatic embryogenesis and calcium alginate encapsulation in *Anethum graveolens* L.: a medicinal herb. Appl Biochem Biotechnol. 173(8):2267-2278.

Rival A, Bertrand L, Beule T, Combes MC, Trouslot P, Lashermes P (1998) Suitability of RAPD analysis for the detection of somaclonal variants in oil palm (*Elaeis guineensis* Jacq). Plant Breed. 117:73-76.

Shah K, Sareeta N (2012) Heat exposure alters the expression of SOD, POD, APX and CAT isozymes and mitigates low cadmium toxicity in seedlings of sensitive and tolerant rice cultivars. Plant Physiol Biochem. 57:106-113.

Shekhawat GS, Verma K, Jana S, Singh K, Teotia P, Prasad A (2010) In vitro biochemical evaluation of cadmium tolerance mechanism in callus and seedlings of *Brassica juncea*. Protoplasma. 239:31-38.

Singla B, Tyagi AK, Khurana JP, Khurana P (2007) Analysis of expression profile of selected genes expressed during auxin-induced somatic embryogenesis in leaf base system of wheat (*Triticum aestivum*) and their possible interactions. Plant Mol Biol. 65(5):677-692.

Sivanesan I, Lim MY, Jeong BR (2011) Somatic embryogenesis and plant regeneration from leaf and petiole explants of *Campanula punctata* Lam. var. rubriflora Makino. Plant Cell Tissue Organ Cult. 107:365-369.

Skůpa P, Opatrný Z, Petrášek J (2014) Auxin biology: Applications and the mechanisms behind. In: Nick P, Opatrny Z (eds) Applied Plant Cell Biology. Springer Berlin Heidelberg. 22:69-102.

Soni M, Kaur R (2014) Rapid in vitro propagation, conservation and analysis of genetic stability of *Viola pilosa*. Physiol Mol Biol Plants. 20:95-101.

Tian M, Gu Q, Zhu M (2003) The involvement of hydrogen peroxide and antioxidant enzymes in the process of shoot organogenesis of strawberry callus. Plant Sci. 165(4):701-707.

Tiryakioglu M, Eker S, Ozkutlu F, Husted S, Cakmak I (2006) Antioxidant defense system and cadmium uptake in barley genotypes differing in cadmium tolerance. J Trace Elem Med Biol. 20(3):181-189.

Wang W, Zhao X, Zhuang G, Wang S, Chen F (2008) Simple hormonal regulation of somatic embryogenesis and/or shoot organogenesis in caryopsis cultures of *Pogonatherum paniceum* (Poaceae). Plant Cell Tiss Org Cult. 95(1):57-67.

Wang WB, Kim YH, Lee HS, Kim KY, Deng X P, Kwak SS (2009) Analysis of antioxidant enzyme activity during germination of alfalfa under salt and drought stresses. Plant Physiol Biochem. 47(7):570-577.

Yeung EC (1995) Structural and developmental patterns in somatic embryogenesis. In: Thorp TA (ed) In vitro embryogenesis in plants. Kluwer Academic, Dordrecht. 20:205-247.

Zhang SG, Han SY, Yang WH, Wei HL, Zhang M, Qi LW (2010) Changes in H_2O_2 content and antioxidant enzyme gene expression during the somatic embryogenesis of *Larix leptolepis*. Plant Cell Tiss Org Cult. 100(1):21-29.